doi:10.1016/j.jmb.2007.12.023 J. Mol. Biol. (2008) 376, 1251–1259

JMB

Available online at www.sciencedirect.com

ScienceDirect

ELSEVIER

Torque–Speed Relationships of Na^+-driven Chimeric Flagellar Motors in *Escherichia coli*

Yuichi Inoue[1], Chien-Jung Lo[2], Hajime Fukuoka[1], Hiroto Takahashi[1], Yoshiyuki Sowa[2], Teuta Pilizota[2], George H. Wadhams[3], Michio Homma[4], Richard M. Berry[2] and Akihiko Ishijima[1]*

[1]*Institute of Multidisciplinary Research for Advanced Materials, Tohoku University, Katahira, Aoba-ku, Sendai 980-8577, Japan*

[2]*Clarendon Laboratory, Department of Physics, University of Oxford, Parks Road, Oxford OX1 3PU, UK*

[3]*Department of Biochemistry, University of Oxford, South Parks Road, Oxford OX1 3QU, UK*

[4]*Division of Biological Science, Graduate School of Science, Nagoya University, Furo-cho, Chikusa-ku, Nagoya 464-8602, Japan*

Received 12 October 2007; received in revised form 10 December 2007; accepted 11 December 2007
Available online 15 December 2007

Edited by J. Karn

The bacterial flagellar motor is a rotary motor in the cell envelope of bacteria that couples ion flow across the cytoplasmic membrane to torque generation by independent stators anchored to the cell wall. The recent observation of stepwise rotation of a Na^+-driven chimeric motor in *Escherichia coli* promises to reveal the mechanism of the motor in unprecedented detail. We measured torque–speed relationships of this chimeric motor using back focal plane interferometry of polystyrene beads attached to flagellar filaments in the presence of high sodium-motive force (85 mM Na^+). With full expression of stator proteins the torque–speed curve had the same shape as those of wild-type *E. coli* and *Vibrio alginolyticus* motors: the torque is approximately constant (at ~2200 pN nm) from stall up to a "knee" speed of ~420 Hz, and then falls linearly with speed, extrapolating to zero torque at ~910 Hz. Motors containing one to five stators generated ~200 pN nm per stator at speeds up to ~100 Hz/stator; the knee speed in 4- and 5-stator motors is not significantly slower than in the fully induced motor. This is consistent with the hypothesis that the absolute torque depends on stator number, but the speed dependence does not. In motors with point mutations in either of two critical conserved charged residues in the cytoplasmic domain of PomA, R88A and R232E, the zero-torque speed was reduced to ~400 Hz. The torque at low speed was unchanged by mutation R88A but was reduced to ~1500 pN nm by R232E. These results, interpreted using a simple kinetic model, indicate that the basic mechanism of torque generation is the same regardless of stator type and coupling ion and that the electrostatic interaction between stator and rotor proteins is related to the torque–speed relationship.

Keywords: rotary motor; flagellar motor; torque generation; torque–speed relationship; chimeric motor

Introduction

The bacterial flagellar motor is a rotary molecular machine that allows many species of bacteria to swim.[1,2] The motor is powered by the flow of ions, H^+ in *Escherichia coli* and Na^+ in marine *Vibrio* species, driven by an inward-directed electrochemical gradient across the cytoplasmic membrane. Rotation is driven by an ensemble of up to ~11 torque-generating stators[3] containing the proteins MotA and MotB in the H^+-driven motor of *E. coli* and PomA and PomB in the Na^+-driven motor of *Vibrio alginolyticus*.[1,2] The torque–speed relationship is an important test of models of the motor mechanism as it allows quantitative comparisons between predictions of models and experimental data. It has been measured using electrorotation[4,5] or optical tweezers[6] to apply external torque to tethered cells and by varying the viscous load either in swimming cells,[7] or with polystyrene beads attached to truncated flagellar stubs.[8,9] A common feature of the

*Corresponding author. E-mail address: ishijima@tagen.tohoku.ac.jp

Abbreviation used: smf, sodium-motive force.

torque–speed relationships of *E. coli* and *V. alginolyticus* is a sharp knee between a "plateau" of nearly constant torque at low speeds and a much steeper linear decrease of torque with speed at higher speeds. At room temperature the knee is at ~175 Hz in *E. coli* and at ~450 Hz in *V. alginolyticus*, and the zero-torque speeds are ~350 and ~700 Hz, respectively. In *E. coli*, the knee speed and zero-torque speed are temperature dependent, but the plateau torque is not.[4,8] Plateau torques appear to vary widely between species, from ~3800 pN nm in *V. alginolyticus*, through ~1300 pN nm in *E. coli* (in the most recent estimate[3]), down to ~350 pN nm in *Caulobacter crescentus*.[7] Torque–speed curves have also been measured for *E. coli* motors containing low numbers of stators.[10] Single-stator motors operated in the plateau regime up to the highest speeds measured, ~100 Hz, and the knee speed in motors with two to five stators appeared to be the same as in motors with a full stator complement. In *C. crescentus*, motors operated in the plateau regime up to the highest speeds measured, ~320 Hz.[7] The knee typically corresponds to the speed at which the output power of the motor is maximum. Different values of knee speed and plateau torque in different species may reflect different modes of swimming or different ion-motive forces, whereas the common shape of the torque–speed curve probably indicates that the basic mechanism of the motor is the same in all species.

A recent breakthrough in experimental investigations of the flagellar motor was the observation of 26 angular steps per revolution in the rotation of a Na^+-driven chimeric motor in *E. coli* with a stator composed of PomA from *V. alginolyticus* and the PomB/MotB fusion protein, PotB.[11] The ability to control the speed of the chimeric motor *via* the sodium-motive force (smf), which is less tightly constrained in *E. coli* than the proton-motive force, is likely to make it an important tool in future investigations of the mechanism of the flagellar motor. Therefore, it is important to characterize its mechanical properties, such as the torque–speed relationship.

Electrostatic interactions that are important for motor rotation in *E. coli* have been demonstrated between two conserved charged residues in the cytoplasmic domain of MotA (Arg90 and Glu98) and conserved charged residues in the rotor protein FliG.[12] The corresponding residues in PomA (Arg88 and Glu96) are less important in *V. alginolyticus*,[13,14] but regain their importance when PomA is part of the chimeric PomA/PotB stator in *E. coli*.[15] Furthermore, PomA contains additional charged residues, such as Arg215 and Arg232 in the cytoplasmic domain, which appear to be important for rotation of Na^+-driven motors.[15] Measuring the torque–speed relationships of a range of mutants in these cri132#?>tical residues will allow detailed inferences to be made about their effect on the rotor–stator interactions that underlie torque generation in the flagellar motor.

In this study we measured torque–speed relationships of the Na^+-driven chimeric PomA/PotB motor in *E. coli*. The torque–speed relationship with a full complement of stators was the same shape as those of wild-type H^+- and Na^+-driven motors, with a plateau torque close to that of the *E. coli* motor and knee and zero-torque speeds close to those of the *V. alginolyticus* motor. Torque–speed relationships with low numbers of stators were consistent with previous measurements of the *E. coli* motor. We also obtained the first torque–speed curves of motors containing mutations in critical charged residues, demonstrating that these mutations affect the knee and zero-torque speeds and the plateau torque in different ways.

Results

Torque–speed relationship with full induction of stator proteins

We measured the speed of polystyrene beads attached to truncated flagellar filament stubs using back focal plane interferometry as described elsewhere.[10] The torque generated by the motor can be estimated as $M=(f_b+f_f)\omega$, where f_b and f_f are rotational frictional drag coefficients of the bead and the filament stub, respectively, and ω is angular velocity. f_b can be estimated as $f_b=8\pi\eta r_b{}^3+6\pi\eta r_b r_r{}^2=g_b\eta$,[10] where r_b and r_r are the radius and the rotational eccentricity of the bead, η is the viscosity of the medium and g_b collects all parameters other than η that affect f_b. Assuming no change of orientation of bead and filament with motor speed,[3] g_b is a constant for each bead on a particular motor. Because the length and orientation of the filament stub is unknown, we need to estimate f_f to obtain an accurate estimate of M. Figure 1a shows the speed *versus* time of a 0.36-μm bead attached to a chimeric motor with full induction of stator proteins, in motility buffer with concentrations 0–13% (w/v) of the viscous agent Ficoll.[8] As the Ficoll concentration increased, the speed decreased from ~600 to ~120 Hz. The speed recovered when the medium was exchanged back to motility buffer without Ficoll, indicating that the motor was not permanently altered by the medium exchanges. Figure 1b shows preliminary estimates of the torque *versus* speed using the equation $M=f_b\omega$, which underestimates M due to the neglect of f_f. The filled square shows the preliminary estimate from fifteen 1-μm polystyrene beads and no Ficoll; the other points are from five different 0.36-μm beads and various Ficoll concentrations as in Fig. 1a. All estimates for a given bead underestimate the true torque by the same factor, $R=f_b/(f_b+f_f)=g_b/(g_b+g_f)$, where $f_f=g_f\eta$ and the geometric factor for filament drag, g_f, is assumed to be constant. A value of g_f can be obtained by equating the plateau torques measured at low speed by 1-μm beads without Ficoll and by 0.36-μm beads with 13% Ficoll:

$$(g_{b1}+g_f)\eta_1\omega_1=(g_{b2}+g_f)\eta_2\omega_2, \qquad (1)$$

where g_{b1} and g_{b2} are the geometric factors of 1- and 0.36-μm beads, η_1 ($=9.86\times10^{-4}$ Pa s) and η_2

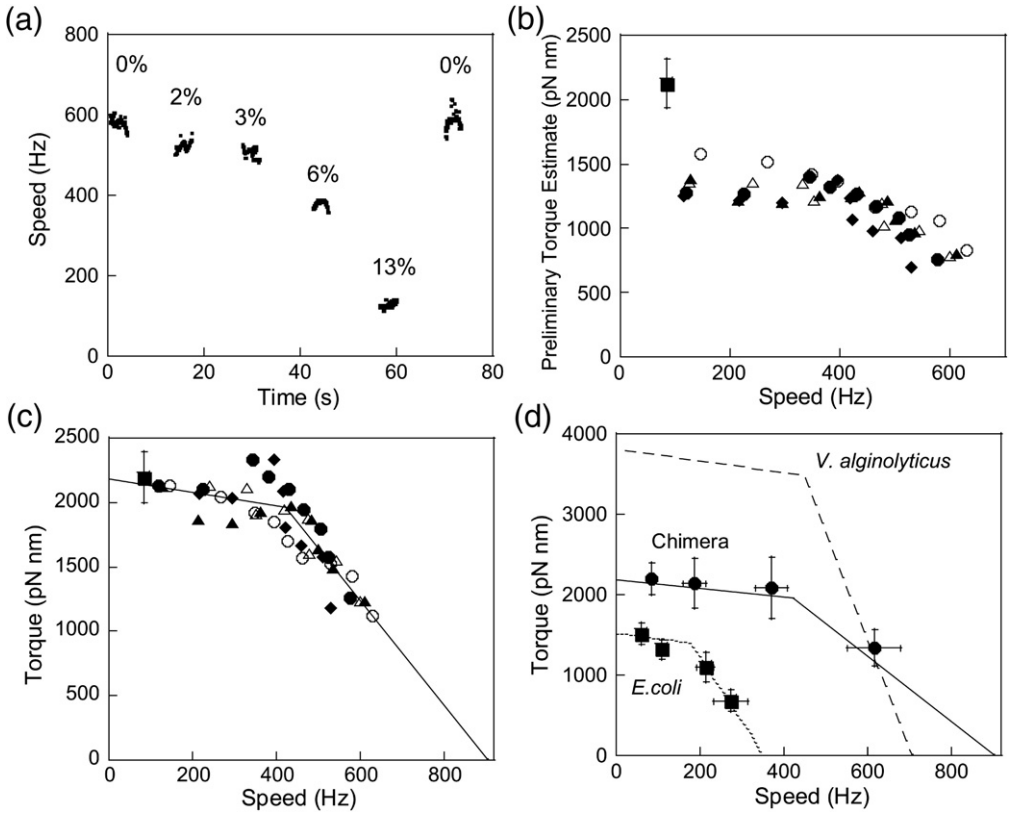

Fig. 1. Torque–speed relationships with fully induced stators. (a) Speed *versus* time of a single chimeric motor measured using a 0.36-μm (diameter) bead in media containing 0–13% (w/v) of the viscous agent Ficoll. (b) Preliminary torque estimates *versus* speed, neglecting the contribution of filament drag, using fifteen 1-μm beads without Ficoll (squares, mean±SD) and 5 individual 0.36-μm beads in 0%, 2%, 3%, 4%, 5%, 6%, 7%, 9% and 13% Ficoll (one symbol for each bead). (c) Corrected torque *versus* speed, using the method described in the text. The average filament drag coefficient without Ficoll was estimated as 0.80±0.20 pN nm s/rad (mean±SD). The torque–speed curve was fitted by two straight lines with an intersection at 421 Hz. (d) Comparison of the torque–speed relationships of different flagellar motors, estimated using four different bead sizes without Ficoll. Measured speeds and estimated torques of chimeric motors (circles) and the H^+-driven *E. coli* motor (squares), using the average filament drag coefficient from (c) (mean±SD). Continuous line: the fitted line for the chimeric motor in (c). Dotted line: published torque–speed relationship,[8] assuming the zero-speed torque is similar to the torque with 1-μm beads. Dashed line: published torque–speed relationship for *V. alginolyticus* motors.[9] Beads (10–18) of each size were measured for each motor.

($=8.18\times10^{-3}$ Pa s) are viscosities at 0% and 13% Ficoll, and ω_1 and ω_2 are speeds measured with 1-μm beads without Ficoll and 0.36-μm beads with 13% Ficoll, respectively. Rearranging Eq. (1) gives

$$g_f = \frac{g_{b2}\eta_2\omega_2 - g_{b1}\eta_1\omega_1}{\eta_1\omega_1 - \eta_2\omega_2}. \qquad (2)$$

We used the data shown in Fig. 1a and b to estimate g_f separately for each of the five 0.36-μm beads measured with Ficoll [$\omega_1 = 84.0\pm6.5$ Hz, $g_{b1} = (4.09\pm0.49)\times10^9$ nm^3, five separate pairs of values of ω_2 and g_{b2}). The average value was $g_f = (1.29\pm0.32)\times10^8$ nm^3, comparable to g_{b2} values, and the corresponding R values for the 0.36-μm beads ranged from 0.59 to 0.74 with average 0.64±0.06 (mean±SD). For 1-μm beads we found $R = 0.97\pm0.01$; the filament drag is very small compared to the drag of 1-μm beads. Figure 1c shows corrected torques equal to the preliminary torques divided by R, using the same symbols as in Fig. 1b. The corrected torque–speed relationship was fitted by two straight lines, following previous reports of the flagellar motor torque–speed relationship,[8,9] with a maximum torque of ~2200 pN nm, a zero-torque speed of ~910 Hz and a knee speed of ~420 Hz.

Rotational speed of the chimeric motor was also measured with four different sizes of beads without Ficoll. In Fig. 1d, torque was calculated by $M = (f_b + f_f)\omega$, using the average value of g_f (above) to estimate $f_f = 0.80\pm0.20$ (pN nm s/rad) for all bead sizes. The torque–speed relationship measured in this way (circles) was consistent with the fitted line of Fig. 1c (continuous line), validating this simpler method. Further validation was obtained by comparing the torque–speed curve of the wild-type *E. coli* motor measured using the same method (Fig. 1d, squares) to published results (dotted line).[8]

Torque–speed relationships with low numbers of stators

Figure 2 shows the speed *versus* time of motors attached to beads of diameter 1, 0.55 and 0.36 μm

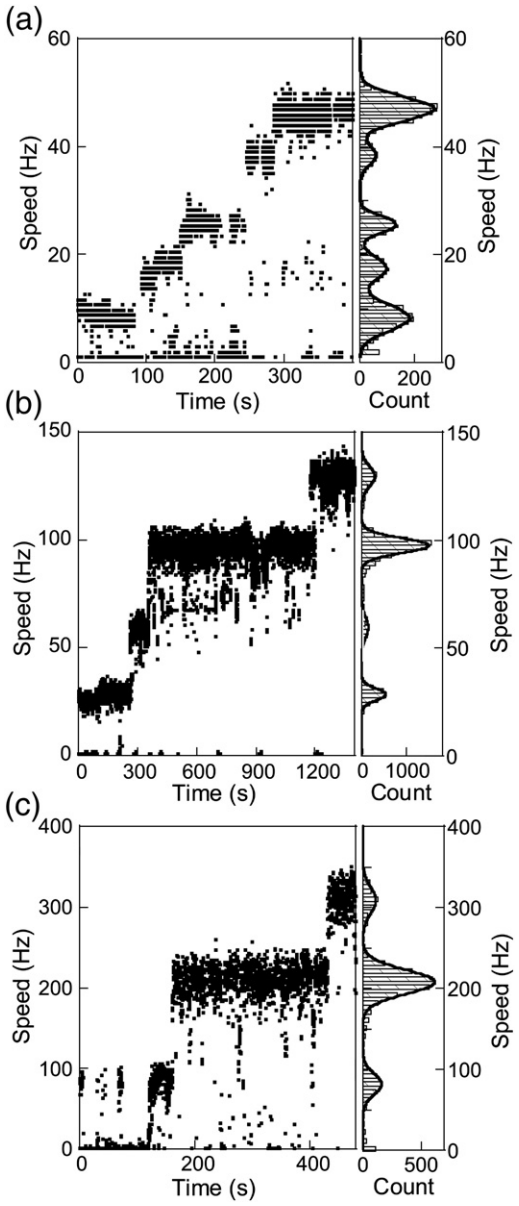

Fig. 2. Resurrection experiments. Speed *versus* time (left) and speed histograms (right) for individual 1- (a), 0.55- (b) and 0.36-μm (c) beads attached to chimeric motors after induced expression of stator proteins. Continuous lines are multiple Gaussian fits.

(Fig. 2a, b and c, respectively), following the induction of stator proteins. Speed increments correspond to successive incorporation of torque-generating stators, a process known as "resurrection."[3,10,16] Speed levels during resurrection were obtained by fitting a multiple Gaussian distribution to speed histograms (Fig. 2a–c, right) and plotting against level number in Fig. 3a. With 0.55- and 1-μm beads, the speed increased linearly with speed level (Fig. 3a, filled triangles and circles), extrapolating to the fully induced speed at approximately level 11 (open triangle and circle). This confirms that the chimeric motor, like the H^+-driven wild-type motor, can contain up to ~11 torque-generating units[3] and that each generates the same torque at speeds below the knee. With 0.36-μm beads, the speed increase was almost linear for 1–5 levels (filled squares), but a saturating fit was required to include the measured fully induced speed at level 11 (open square). Assuming that the number of stators in a fully induced motor does not depend on bead size, this result is consistent with the measured reduction in motor torque at speeds above the knee at ~420 Hz. Figure 3b shows torque–speed relationships of

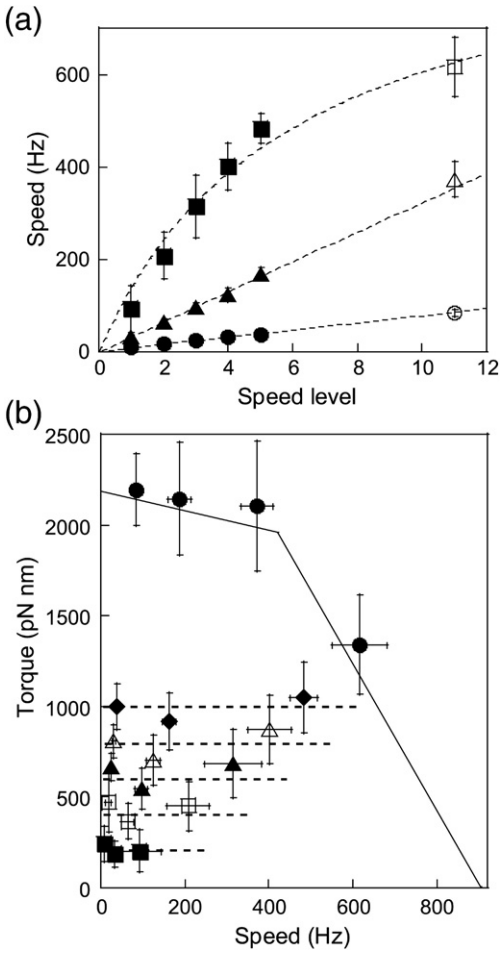

Fig. 3. Torque–speed relationships with low numbers of stators. (a) Speed *versus* level number from resurrection traces (filled symbols). Speeds (mean±SD) were from multiple-Gaussian fitting of speed histograms (Fig. 2, right) of 6–15 resurrections with each bead size 1 μm (circles), 0.55 μm (triangles), and 0.36 μm (squares). Speeds of fully induced motors with the same bead sizes (open symbols) are shown at level 11, which assumes that the number of torque-generating units at full induction is ~11. Dashed lines are linear fits except for 0.36-μm beads, where the Michaelis–Menten equation is used. (b) Torque–speed relationships of motors with 1–5 stators (filled squares, open squares, filled triangles, open triangles and diamonds, respectively) calculated using the data of (a) and the filament drag coefficient in Fig. 1c. The torque–speed relation for fully induced motors is reproduced from Fig. 1d for comparison (filled circles). Dashed lines are drawn at intervals of 200 pN nm to guide the eye.

motors with one to five stators (filled squares, open squares, filled triangles, open triangles and diamonds, respectively) calculated using the data of Fig. 3a and the method of Fig. 1d. The torque–speed relation for fully induced motors is reproduced from Fig. 1d for comparison (filled circles). Torque increased in proportion to the number of stators, and for each stator number torque was approximately constant over the range of measured speeds, up to ~100 Hz per stator. Note in particular that the knee speed in four- and five-stator motors is not significantly slower than in the fully induced motor.

Torque–speed relationships of motors with PomA mutations

Conserved arginines at positions 88 and 232 in the cytoplasmic domain of PomA have been shown to be important for torque generation in the chimeric motor.[15] Their approximate locations are illustrated in Fig. 4a, which also indicates putative interactions with charged residues on FliG. R88 corresponds to the conserved residue R90 in *E. coli* MotA; R232 is a charged residue near the C-terminus of PomA with no corresponding residue in *E. coli*. Chimeric motors with the point mutations R88A or R232E in PomA were reported as totally deficient in swarming on soft agar and weakly swimming in liquid media.[15] We repeated these experiments using the host strain RP6894 in which *motAmotB* is deleted and flagellar filament and rotor proteins are wild type.[17] Our results were the same as those reported previously except we found that R88A showed normal rather than weak swimming (Fig. 4b), perhaps as a consequence of expressing FliG from the chromosome rather than from a plasmid as in the previous work.[15] Figure 4c shows torque–speed curves for chimeric motors with fully expressed PomA, either wild type (circles) or with mutations R88A (triangles) or R232E (squares). The method and filament drag coefficients are the same as for Fig. 1d, but the host strain is different. Sticky flagellar filaments were expressed from plasmid pYS11 in host strain YS34 in the experiments of Figs. 1–3, but from the chromosome in host strain JHC36 in the experiments of Fig. 4c. The torque–speed relationship of the wild-type PomA motor reconstituted in JHC36 (Fig. 4c, circles) was indistinguishable from that of the same motor in YS34 (Fig. 1d), demonstrating that this change of host strain does not alter the motor. At low speeds the mutation R232E reduces the torque to ~65%, whereas R88A causes little change. At high speeds both mutations reduce the torque substantially and the zero-torque speed is reduced from ~910 to ~400 Hz. These results indicate that both mutations slow the mechanism of the motor and that R232 has an additional effect in reducing the torque at low speeds. The lines in Fig. 4c are torque–speed curves predicted by a simple kinetic model for the wild-type and mutant motors (see Discussion).

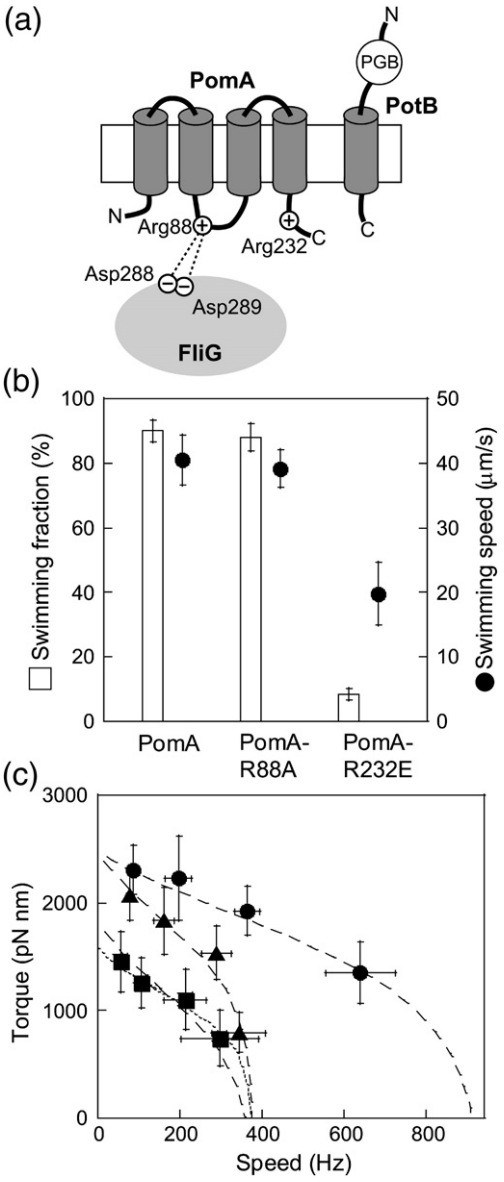

Fig. 4. Chimeric motors with point mutations in PomA. (a) A sketch of the topology of PomA and PotB, showing the locations of conserved charged residues R88 and R232 in PomA and putative interactions with the rotor protein FliG. (b) Swimming of cells with PomA point mutations. Chimeric stators with no mutation, R88A, or R232E in PomA were expressed in RP6894, a strain with normal flagellar filament and rotor. Fractions of cells swimming (mean±SD, left axis) are shown as bars, speeds of swimming cells (mean±SD, right axis) as circles. (c) Torque–speed relationships. The same PomA variants as in b were expressed in JHC36, a strain with sticky flagellar filaments expressed from the chromosome. Torque-speed curves were measured using the method and filament drag coefficients of Fig. 1d. Circles, chimeric motor; triangles, chimeric motor with R88A; squares, chimeric motor with R232E. Speeds were measured in 10–20 cells from two to three separate cultures. Fitted lines are torque–speed curves predicted by a simple kinetic model (Fig. 5 and Table 1). For PomA-R88A the three parameter sets of Table 1 gave indistinguishable fits, so only the fit for the parameters in the rightmost column is shown (dashed line). For PomA-R232E, fits with reduced numbers of ions (N, dotted line) or reduced membrane potential ($\Delta\Psi$, dashed line) are shown.

Discussion

The torque–speed relationship of the chimeric motor has the same shape as those of the wild-type motors of *E. coli* and *V. alginolyticus* (Fig. 1d), suggesting that all three motors share the same basic mechanism for torque generation. In particular, our Ficoll experiments demonstrate that the Na^+-driven chimera shows the same sharp knee (Fig. 1c) between the plateau and high-speed domains as the H^+-driven *E. coli* motor, a feature that is not easily predicted by models of the motor mechanism.[5,18] The Na^+-driven motors are faster, with knee and zero-torque speeds approximately double those of the H^+-driven motor, which is further slowed when H^+ is replaced by deuterium.[19] These observations suggest that the rate-limiting step in the mechanochemical cycle of torque generation at low load is related to ion transfer.

The plateau torque of the chimera was ~2200 pN nm, compared to ~3800 and ~1500 pN nm for *V. alginolyticus* and *E. coli* motors, respectively (Fig. 1d). The values for the chimera and *E. coli* motors are consistent with previous results using 1-μm beads.[3] Considering the balance between input energy (number of ions × ion-motive force) and output work (2π × torque), the minimum number of ions required per revolution of the *E. coli* motor was previously estimated as 38±11 per stator.[3] A similar calculation using the measured smf in *E. coli* (−187 mV[20]) yields a similar result for the chimeric motor (42±4 per stator). The plateau torque reported for *V. alginolyticus* is 1.7 times larger than that of the chimeric motor, which is difficult to explain. Excluding the possibility of experimental error, we might speculate that the diameter of the motor is larger, which would increase both the number of stators and the number of ions used per stator per revolution (presumably proportional to the periodicity of the rotor). Increasing both of these numbers, and also the smf, by a factor of 1.2 would account for the larger torque compared to *E. coli*. The chimeric motor has been observed to take 26 steps per revolution when driven by a presumed single stator at low smf.[11] Thus, it is just possible within the limits of experimental error that a single ion might drive a single step of this size in the chimera and *E. coli* motors, but the *V. alginolyticus* motor would need either to take smaller steps or to use more ions per step. If all three types of motors do indeed use two or more ions per step, then the increased torque of the *V. alginolyticus* motor could be explained by greater efficiency, although it seems unlikely that the *E. coli* motor would be less than half as efficient as that of *V. alginolyticus*. The additional motor proteins, MotX and MotY, in *V. alginolyticus* might have some role to play, but these questions will only be resolved with further experimental investigation.

Our measurements of torque and speed in resurrection experiments are consistent with previous results using the *E. coli* motor:[10] the shape of the torque–speed curve appears to be independent of stator number. Thus, it appears that in the chimera, as previously inferred for the wild-type motor, the stators work with a high duty ratio and there exists a rate-limiting step in the mechanochemical cycle of each stator that cannot be speeded up by the torque transmitted from other stators *via* the rotor.

Our measurements of torque–speed curves of single flagellar motors with mutations in critical charged residues of PomA represent an improvement over the swarming and swimming assays that are used to discover and classify these mutations.[15] Swarm assays are dependent upon growth and chemotaxis[21] and the relationship between swimming and motor rotation is complicated by the formation of flagellar bundles in *E. coli*.[22] The mutations R88A and R232E leave the shape of the torque–speed curve essentially unchanged, although the slope in the plateau region may be steeper, and the ratio of knee- to zero-torque speeds larger, than with wild-type PomA. Both mutations reduce the zero-torque speed to ~400 Hz, indicating that they slow the rates of transitions in the mechanochemical cycle. R232E also reduces the plateau torque to about ~65%. Several explanations for this are possible. Perhaps the simplest is that the number of stators in a fully induced motor is reduced by this mutation, indicating a role for R232 in stator assembly. Independent evidence for a connection between torque generation and stator assembly already exists: stators detach from the motor when it is stopped by de-energization.[11,23,24] However, our preliminary experiments with expressing low levels of stators suggest that the motor can be equipped with 11 R232E chimeric stators and the speed per stator is reduced by R232E mutation (data not shown). Thus, alternatives other than stator number may be required for the explanations. It is possible that the coupling ratio (fewer ions per revolution) or efficiency (ion flow without torque generation) could be altered, for example, by slippage between the rotor and stator, or the smf could be reduced because ion leakage through the mutant: expression of chimeric stators has been shown to increase the internal Na^+ concentration in *E. coli*,[25] indicating that the ion flux through a chimeric motor is sufficient to alter the smf in *E. coli*. Further experiments will be needed to distinguish between these alternatives.

We used a simple kinetic model of the motor mechanism to calculate torque–speed curves for comparison to the data. The kinetic scheme of the model, which was originally proposed by Iwazawa *et al.*[26] and was used to fit the *V. alginolyticus* data,[9] is reproduced in Fig. 5. Rate constants k_1–k_4 describe Na^+ exchange with the external and cytoplasmic media, k_0 a conformational change that changes which side of the membrane accesses the Na^+-binding site, and k_A, k_B the equivalent conformational change with Na^+ bound. The model assumes that the conformational change with Na^+ bound is entirely responsible for tight coupling between charge translocation across the membrane and rotation, so that only the rate constants k_A and k_B

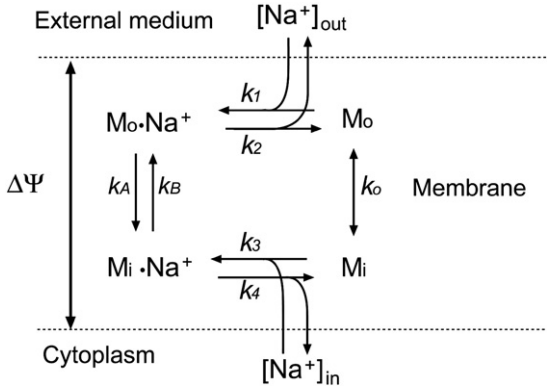

Fig. 5. A simple kinetic model of the mechanochemical cycle of torque generation[9,26] was used to understand the effect of mutation on the torque–speed relationship of the chimeric motor. Parameters used to fit the data of Fig. 4c are shown in Table 1. See the text for details.

depend upon membrane voltage ($\Delta\Psi$) and torque (M). For simplicity, these rate constants are defined as $k_A = k_0 \exp[-(2\pi M/N + e\Delta\Psi)/2kT]$ and $k_B = k_0 \exp[(2\pi M/N + e\Delta\Psi)/2kT]$, where k is Boltzmann's constant, e is the elementary charge, T is the absolute temperature and N is the number of ions coupled to each revolution of the motor. These expressions automatically satisfy detailed balance, which further requires $(k_1k_4)/(k_2k_3) = 1$. Thus, the model has five free parameters (N, k_0, and any three out of k_1–k_4) in addition to M, $\Delta\Psi$ and the internal and external Na^+ concentrations (Table 1).

Using the parameter values listed in Table 1, the model predicts torque–speed curves that capture the concave-down shape of the experimental results and the differences between the different PomA variants (Fig. 4c). Tight-coupled models of this type have not been able to predict the sharp knee in the torque–speed curve,[5] but by virtue of their simplicity compared to more detailed models[18] they are a useful tool to understand the broad features of the torque–speed relationship. The reduced speed of motors with mutations can be fitted in three different ways: by reducing rates of Na^+ binding and dissociation (k_1–k_4) 15-fold (right column for PomA-R88A in Table 1, dashed line in Fig. 4c), by reducing the rate of conformational changes (k_0) 2.5-fold (middle column), or by reducing all rates (k_0–k_4) 2.3-fold (left column). Thus, the electrostatic interaction between PomA and FliG affects the rate-limiting step in torque generation at low load, but we cannot distinguish between changes in ion binding and the rates of conformational changes without further measurements of torque–speed curves with different sodium concentrations and membrane voltages. The reduced plateau torque of the R232E mutation was fitted by decreasing either N by ~37% (dotted line) or $\Delta\Psi$ by ~36% (dashed line): the model cannot distinguish between the possible mechanisms for this reduction, although our preliminary experiments favour the reduction of $\Delta\Psi$, as discussed above. Further torque–speed measurements of mutant chimeric motors will allow a detailed investigation of the electrostatic interactions between stator and rotor proteins that are essential for torque generation in the flagellar motor.

Materials and Methods

Chemicals

Ficoll 400 (dialyzed and lyophilized) was from Sigma Chemical Co. (St. Louis, MO). Polystyrene latex beads (diameter 1.053±0.010, 0.771±0.025, 0.548±0.016 and 0.356±0.014 μm; 2.6% solids) were from Polysciences (Warrington, PA). All other chemicals were reagent grade. Motility buffer was 10 mM potassium phosphate, 85 mM NaCl and 0.1 mM ethylenediaminetetraacetic acid, pH 7.0.

Bacterial strains

Chimeric motors with no mutations on PomA were expressed in *E. coli* strain YS34 (Δ*cheY*, *fliC*: :Tn10, Δ*pilA*, Δ*motAmotB*) with plasmids pYS11 (*fliC*^{sticky}, ampicillin resistance) and pYS13 (*pomApotB*, IPTG inducible, chrolamphenicol resistance) as described.[11] H^+-driven

Table 1

Parameter	PomA	PomA-R88A		PomA-R232E	
$[Na^+]_{out}$ (mM)	85[a]	85		85	
$[Na^+]_{in}$ (mM)	14[b]	14		14	
$\Delta\Psi$ (mV)	−140[c]	−140		−140	−90
N	520[d]	520		330	520
k_0 (s^{-1})	1.2×10^5	5.2×10^4	4.8×10^4	1.2×10^5	1.2×10^5
$k_1=k_3$ (M^{-1} s^{-1})	6.0×10^7[e]	2.6×10^7	6.0×10^7	4.0×10^6	4.0×10^6
$k_2=k_4$ (s^{-1})	6.0×10^5[e]	2.6×10^5	6.0×10^5	4.0×10^4	4.0×10^4
		(k_0–k_4)÷2.3	k_0÷2.5	(k_1–k_4)÷15	Reduce N / Reduce $\Delta\Psi$

Parameters for data fitting with the four-state model (see the text; Figs. 4c and 5). The three sets of rate constants (k_0–k_4) used for the R88A mutation gave very similar torque–speed curves (see the text; Fig. 4c). Further reducing either N or $\Delta\Psi$ gave similar quality fits to the torque–speed curve for the R232E mutation.

[a] Sodium concentration of motility buffer.
[b] From Lo *et al.*[25]
[c] From Lo *et al.*[20]
[d] The number of ions is determined by the stall torque in a tight-coupled model such as this, which has 100% efficiency at stall.
[e] As used for *V. alginolyticus*.[9]

motors were expressed in *E. coli* strain HCB1271 (*fliC*::Tn10, Δ*pil*A′-KnR, *motA448*) with plasmids pDFB36 (*motA*, IPTG inducible, ampicillin resistance) and pDF313Cm (*fliC*^{sticky}, chrolamphenicol resistance) as described.[10] Chimeric motors with PomA mutations[15] were expressed in *E. coli* strain JHC36 (this work). The *fliC*^{sticky} region of strain PS2589 (a gift from Jeffrey Stock, Princeton University) chromosome was amplified using primers that annealed approximately 500 bp upstream and downstream of *fliC*^{sticky}. This PCR fragment was digested with SphI/SacI, ligated into the suicide vector pDS132,[27] sequenced and transformed into electrocompetent strain YS34. Genomic replacement of *fliC* with *fliC*^{sticky} was carried out as described[27] and gene replacement confirmed by Southern blot analysis and PCR. The resultant strain was designated JHC36. Chimeric stators were expressed in JHC36 from plasmids pTH200, pTH201 and pTH202, which are pMMB206 derivatives carrying PomA/PotB, PomA-R88A/PotB,and PomA-R232E/PotB, respectively, inducible by IPTG. For swimming assays, chimeric stators were expressed in strain RP6894 (Δ*motAmotB,* normal flagellar filaments,[17] from plasmids pTH200, pTH201 and pTH202.

Cell culture and stator expression

Cells were grown from frozen stocks with shaking in T broth (1% Bacto tryptone, 0.5% NaCl) containing 25 μg/ml chrolamphenicol and 50 μg/ml ampicillin at 31 °C for 5 h. For full induction of chimeric stator proteins, cells were grown in the presence of 0.05 mM IPTG. For full induction of wild-type H^+ stator proteins, cells were treated with 5 mM IPTG at 25 °C for 3 h after growth at 25 °C to OD_{590} of ~0.4. IPTG concentrations and growth times were selected to give the maximum rotation rate within the ranges tested (0.005–5 mM, 2–8 h). For resurrection experiments cells were grown with 0–0.005 mM IPTG, and resurrections were observed typically within 1 h after application of 0.05–0.9 mM IPTG in motility buffer containing 10% T broth.

Swimming cells

After application of 20 mM serine, which was used to suppress clockwise rotation, cells in T broth were observed for 1 min under a phase-contrast microscope and recorded on a videotape for later analysis. Cells that moved more than 5 μm in 1 s were counted as swimming cells. Cells which moved less than 5 μm in 1 s (due to Brownian motion) were counted as nonswimming cells. Some nonswimming cells showed behavior distinct from Brownian motion, such as very slow swimming due to frequent changes in swimming direction (>1 s^{-1}), rotation of the cell body with the filament stuck to the glass surface, or complete immobilization stuck to the glass surface. Such cells were ~10% of the population for all three motor types and were excluded in this analysis. Swimming fraction was calculated as number of swimming cells divided by the total number of cells that were not excluded from the analysis. Swimming fractions, mean±SD, were estimated from three different cultures. Swimming speeds, mean±SD, were calculated from 60 cells.

Torque–speed measurements

Polystyrene beads were attached to truncated flagella and their position was measured with back focal plane interferometry as described,[10] except using a laser of wavelength 632.8 nm (He–Ne laser, 05LHP-111, Melles Griot, USA) or 1064 nm (diode-pumped solid-state laser, L04-1000S-1064, Elforlight, Northants, UK). Rotational speed was obtained from power spectra of the bead position as described.[3] All experiments were performed at 23 °C.

Torque was calculated as described in the text, using the reported viscosity of a Ficoll solution.[8] The rotational eccentricity of a bead was estimated from the quadrant photodiode signal, calibrated using beads stuck to the surface and moved with a piezoelectric stage (P-517P3CL, Physik Instrumente, Germany).

Tight-coupled model

The speed of the motor at given torque, Na^+ concentrations and ΔΨ was predicted using the four-state model of Fig. 5 as described.[9,26]

Acknowledgements

We thank Prof. David Blair for the gift of the strain RP6894 and Prof. Judith Armitage and Dr. Jennifer Chandler for help with the construction of strain JHC36. This work was supported by Grants-in-Aid for Scientific Research from the Japan Society for the Promotion of Science (A.I.). C.-J.L. thanks Swire Group/ORS for financial support. Y. S. thanks Uehara Memorial Foundation and Murata Overseas Scholarship Foundation for financial support. The research of R.B. was supported by the EPSRC and BBSRC, the Interdisciplinary Research Collaboration in Bionanotechnology and the EU FP6 programme, and of G.W. by the Interdisciplinary Research Collaboration in Bionanotechnology.

References

1. Blair, D. F. (2003). Flagellar movement driven by proton translocation. *FEBS Lett.* **545**, 86–95.
2. Yorimitsu, T. & Homma, M. (2001). Na^+-driven flagellar motor of *Vibrio*. *Biochim. Biophys. Acta*, **1505**, 82–93.
3. Reid, S. W., Leake, M. C., Chandler, J. H., Lo, C. J., Armitage, J. P. & Berry, R. M. (2006). The maximum number of torque-generating units in the flagellar motor of *Escherichia coli* is at least 11. *Proc. Natl Acad. Sci. USA*, **103**, 8066–8071.
4. Berg, H. C. & Turner, L. (1993). Torque generated by the flagellar motor of *Escherichia coli*. *Biophys. J.* **65**, 2201–2216.
5. Berry, R. M. & Berg, H. C. (1999). Torque generated by the flagellar motor of *Escherichia coli* while driven backward. *Biophys. J.* **76**, 580–587.
6. Berry, R. M. & Berg, H. C. (1997). Absence of a barrier to backwards rotation of the bacterial flagellar motor demonstrated with optical tweezers. *Proc. Natl Acad. Sci. USA*, **94**, 14433–14437.
7. Li, G. & Tang, J. X. (2006). Low flagellar motor torque and high swimming efficiency of *Caulobacter crescentus* swarmer cells. *Biophys. J.* **91**, 2726–2734.
8. Chen, X. & Berg, H. C. (2000). Torque–speed relation-

ship of the flagellar rotary motor of *Escherichia coli*. *Biophys. J.* **78**, 1036–1041.
9. Sowa, Y., Hotta, H., Homma, M. & Ishijima, A. (2003). Torque–speed relationship of the Na^+-driven flagellar motor of *Vibrio alginolyticus*. *J. Mol. Biol.* **327**, 1043–1051.
10. Ryu, W. S., Berry, R. M. & Berg, H. C. (2000). Torque-generating units of the flagellar motor of *Escherichia coli* have a high duty ratio. *Nature*, **403**, 444–447.
11. Sowa, Y., Rowe, A. D., Leake, M. C., Yakushi, T., Homma, M., Ishijima, A. & Berry, R. M. (2005). Direct observation of steps in rotation of the bacterial flagellar motor. *Nature*, **437**, 916–919.
12. Zhou, J., Lloyd, S. A. & Blair, D. F. (1998). Electrostatic interactions between rotor and stator in the bacterial flagellar motor. *Proc. Natl Acad. Sci. USA*, **95**, 6436–6441.
13. Yorimitsu, T., Sowa, Y., Ishijima, A., Yakushi, T. & Homma, M. (2002). The systematic substitutions around the conserved charged residues of the cytoplasmic loop of Na^+-driven flagellar motor component PomA. *J. Mol. Biol.* **320**, 403–413.
14. Yorimitsu, T., Mimaki, A., Yakushi, T. & Homma, M. (2003). The conserved charged residues of the C-terminal region of FliG, a rotor component of the Na^+-driven flagellar motor. *J. Mol. Biol.* **334**, 567–583.
15. Yakushi, T., Yang, J., Fukuoka, H., Homma, M. & Blair, D. F. (2006). Roles of charged residues of rotor and stator in flagellar rotation: comparative study using H^+-driven and Na^+-driven motors in *Escherichia coli*. *J. Bacteriol.* **188**, 1466–1472.
16. Blair, D. F. & Berg, H. C. (1988). Restoration of torque in defective flagellar motors. *Science*, **242**, 1678–1681.
17. Braun, T. F., Poulson, S., Gully, J. B., Empey, J. C., Van Way, S., Putnam, A. & Blair, D. F. (1999). Function of proline residues of MotA in torque generation by the flagellar motor of *Escherichia coli*. *J. Bacteriol.* **181**, 3542–3551.
18. Xing, J., Bai, F., Berry, R. & Oster, G. (2006). Torque–speed relationship of the bacterial flagellar motor. *Proc. Natl Acad. Sci. USA*, **103**, 1260–1265.
19. Chen, X. & Berg, H. C. (2000). Solvent-isotope and pH effects on flagellar rotation in *Escherichia coli*. *Biophys. J.* **78**, 2280–2284.
20. Lo, C. J., Leake, M., Pilizota, T. & Berry, R. (2007). Non-equivalence of membrane voltage and ion-gradient as driving forces for the bacterial flagellar motor at low load. *Biophys. J.* **93**, 294–302.
21. Harshey, R. M. (2003). Bacterial motility on a surface: many ways to a common goal. *Annu. Rev. Microbiol.* **57**, 249–273.
22. Darnton, N. C., Turner, L., Rojevsky, S. & Berg, H. C. (2007). On torque and tumbling in swimming *Escherichia coli*. *J. Bacteriol.* **189**, 1756–1764.
23. Armitage, J. P., Ingham, C. & Evans, M. C. (1985). Role of proton motive force in phototactic and aerotactic responses of *Rhodopseudomonas sphaeroides*. *J. Bacteriol.* **161**, 967–972.
24. Fung, D. C. & Berg, H. C. (1995). Powering the flagellar motor of *Escherichia coli* with an external voltage source. *Nature*, **375**, 809–812.
25. Lo, C. J., Leake, M. C. & Berry, R. M. (2006). Fluorescence measurement of intracellular sodium concentration in single *Escherichia coli* cells. *Biophys. J.* **90**, 357–365.
26. Iwazawa, J., Imae, Y. & Kobayasi, S. (1993). Study of the torque of the bacterial flagellar motor using a rotating electric field. *Biophys. J.* **64**, 925–933.
27. Philippe, N., Alcaraz, J. P., Coursange, E., Geiselmann, J. & Schneider, D. (2004). Improvement of pCVD442, a suicide plasmid for gene allele exchange in bacteria. *Plasmid*, **51**, 246–255.